JACC: CARDIOVASCULAR IMAGING
VOL. 8, NO. 6, 2015

ISSN 1936-878X/$36.00
PUBLISHED BY ELSEVIER INC.
http://dx.doi.org/10.1016/j.jcmg.2015.02.009

Right Intraventricular Dyssynchrony in Idiopathic, Heritable, and Anorexigen-Induced Pulmonary Arterial Hypertension

Clinical Impact and Reversibility

Roberto Badagliacca, MD, PhD,* Manuela Reali, MD, PhD,* Roberto Poscia, MD, PhD,* Beatrice Pezzuto, MD,* Silvia Papa, MD,* Mario Mezzapesa, MD,* Martina Nocioni, MD,* Gabriele Valli, MD, PhD,* Elisa Giannetta, MD, PhD,† Susanna Sciomer, MD,* Carlo Iacoboni, MD,* Francesco Fedele, MD,* Carmine Dario Vizza, MD*

ABSTRACT

OBJECTIVES The aim of this study was to determine the prevalence of right intraventricular dyssynchrony, its determinants and prognostic impact in idiopathic, heritable, and anorexigen-induced pulmonary arterial hypertension.

BACKGROUND Right ventricular dyssynchrony has been described in pulmonary arterial hypertension, but no evidence is available on its prognostic impact and evolution after therapy.

METHODS In 83 consecutive therapy-naïve patients, right ventricular dyssynchrony was evaluated by 2-dimensional speckle-tracking echocardiography calculating the standard deviation of the times to peak-systolic strain for the 4 mid-basal right ventricular segments (RV-SD4). After baseline (World Health Organization [WHO] class, pulmonary hemodynamics, 6-min walk test [6MWT]), a second assessment was performed after 12 months or when clinical worsening occurred.

RESULTS Patients with right ventricular dyssynchrony (RV-SD4 >18 ms) had advanced WHO class, worse 6MWT, right ventricular remodeling, and hemodynamic profile compared with patients ≤18 ms. Determinants of dyssynchrony included pulmonary vascular resistance, QRS duration, and right ventricular end-diastolic area ($r^2 = 0.38$; $p < 0.000001$). At 12 months, 32.5% of patients presented clinical worsening (actuarial rates: 19% at 6 months, 31% at 1 year). Multivariable models for clinical worsening prediction showed that the addition of RV-SD4 to clinical and hemodynamic variables (WHO IV, 6MWT, and cardiac index) significantly increased the prognostic power of the model (0.74 vs. 0.81; $p = 0.005$, 95% confidence interval [CI]: 0.02 to 0.11). Receiver operating characteristic analysis identified RV-SD4 ≥ 23 ms as the best cutoff value for clinical worsening prediction (95% negative predictive value). At 12 months, normalization of dyssynchrony was achieved in patients with a large reduction of pulmonary vascular resistance (-42 ± 4%).

CONCLUSIONS Right ventricular dyssynchrony is frequent in pulmonary arterial hypertension, is an independent predictor of clinical worsening, and might regress during effective treatments. (J Am Coll Cardiol Img 2015;8:642–52)

Pulmonary arterial hypertension (PAH) is a severe disease characterized by a progressive elevation of pulmonary vascular resistance (PVR), ultimately resulting in right ventricular (RV) dysfunction leading to heart failure and death (1). Prognosis depends on the ability of the RV to maintain its function in the face of increased afterload (2). Ventricular mechanical dyssynchrony has been well described in left ventricular (LV) failure as an important component of LV systolic performance and has formed the basis of cardiac resynchronization therapy, leading to significant improvements in

From the *Department of Cardiovascular and Respiratory Science, Sapienza University of Rome, Rome, Italy; and the †Department of Experimental Medicine, Sapienza University of Rome, Rome, Italy. The authors have reported that they have no relationships relevant to the contents of this paper to disclose. Drs. Fedele and Vizza are joint last authors.

Manuscript received November 26, 2014; revised manuscript received February 6, 2015, accepted February 12, 2015.

patient functional capacity and survival (3). Although RV mechanical dyssynchrony (RVD) has recently been described in pulmonary hypertension (4–6), currently we do not have evidence on its prognostic relevance. To address this issue, RV mechanics should be evaluated taking into account several methodological considerations such as a larger and more homogeneous PAH population than previous studies, absence of confounding factors, adequate management and follow-up of patients, and application of new echocardiographic techniques for mechanical delay evaluation.

Accordingly, the aims of this study were to determine the prevalence of RVD in a large cohort of idiopathic, heritable, and anorexigen-induced pulmonary arterial hypertension (IPAH, HPAH, APAH), therapy-naïve patients, to better elucidate the factors influencing RVD, to evaluate the prognostic impact of RVD and its evolution on long-term follow-up.

METHODS

POPULATION AND STUDY PROTOCOL. The study population included 83 consecutive therapy-naïve patients with IPAH, HPAH, and APAH, without severe tricuspid regurgitation or electrocardiographic signs of intraventricular conduction delay to avoid other confounding factors for RVD evaluation. Patients were referred to our center from January 1, 2010 to December 31, 2011, and diagnosis of PAH had been made according to European guidelines (7). Three patients with suboptimal echocardiographic images were excluded from all subsequent analyses. Thus, the patient study group consisted of 80 patients.

SEE PAGE 653

Patients with IPAH, HPAH, and APAH should be considered a homogeneous population with common pathophysiological pathways and histologic findings (8).

Baseline evaluation included medical history, physical examination, a nonencouraged 6-min walk test (6MWT), right heart catheterization (RHC), and echocardiographic assessment. Thereafter, patients started a specific PAH treatment, according to European guidelines (7).

All patients were prospectively followed-up for 12 months with phone calls (every month) and clinical examinations (every 1 to 3 months) for the presence of clinical worsening (CW), defined as a reduction in exercise capacity (-15% compared with baseline 6MWT), worsening in World Health Organization (WHO) functional class, or clinical deterioration requiring hospital admission (need for intravenous diuretic or inotropic drugs, need for new PAH therapies, lung transplantation, or death) (9). The CW was evaluated by 2 physicians (V.C.D., P.R.) blinded on the echocardiographic results.

A second assessment (WHO class, 6MWT, RHC, echocardiography) was performed after 12 months or when CW occurred. All patients were included in the study protocol after informed consent. The protocol was approved by the Institutional Review Board for human studies of the Policlinico Umberto I-Sapienza University of Rome (Protocol n. 42412).

RIGHT HEART CATHETERIZATION. Hemodynamic evaluation was made with standard technique, as previously described (10).

STANDARD ECHOCARDIOGRAPHY. Echocardiographic studies were performed using commercially available equipment (Vivid S6, GE Medical Systems, Milan, Italy) and acquired within 24 hours from RHC. Standard M-mode, 2-dimensional (2D) and Doppler images were obtained during breath hold and stored in cine-loop format from 3 consecutive beats. Measurements were performed in accordance with the American Society of Echocardiography Guidelines (11).

The following parameters and derived measures were considered in the analysis: right atrial area (RA area), right ventricular end-diastolic area (RVEDA), right ventricular end-systolic area (RVESA), right ventricular fractional area change (RVFAC) % (RVFAC = [RVEDA - RVESA]/RVEDA × 100), tricuspid annular plane systolic excursion (TAPSE), left ventricular systolic eccentricity index (LVEIs) and left ventricular diastolic eccentricity index (LVEId), and presence of pericardial effusion.

Pulsed-wave tissue Doppler imaging (PW-TDI) was used for the following measures: isovolumic contraction velocity (S1), isovolumic acceleration (IVA), and peak systolic velocity (S2). All reported measurements are the averages derived from 3 consecutive cardiac cycles.

2D SPECKLE-TRACKING ECHOCARDIOGRAPHY. Acquisition. For speckle tracking analysis (EchoPAC workstation 7.0.1, GE Medical Systems), standard grayscale 2D images in the 4-chamber apical view were acquired and digitally stored in 3 beats cine-loop format.

Analysis. To assess the segmental characteristics of the RV, we adopted the 6-segment model, excluding the apical segments for the analysis because of the

ABBREVIATIONS AND ACRONYMS

IVA = isovolumic acceleration

IVS = interventricular septum

LVEId = left ventricular diastolic eccentricity index

LVEIs = left ventricular systolic eccentricity index

PW-TDI = pulsed waved tissue Doppler imaging

RV = right ventricular

RVEDA = right ventricular end-diastolic area

RVESA = right ventricular end-systolic area

RVFAC = right ventricular fractional area change

RVFW = right ventricular free wall

RV-SD4 = standard deviation of the times to peak-systolic strain for the 4 mid-basal right ventricular segments

S1 = isovolumic contraction velocity

S2 = peak systolic velocity

STE = speckle-tracking echocardiography

high variability of that segments observed even in normal subjects. This decision is supported by software-related technical issues (12).

To quantify right intraventricular dyssynchrony, we considered longitudinal strain and calculated the standard deviation of the times to peak-systolic strain for the 4 mid-basal RV segments corrected to the R-R interval between 2 QRS complexes, according to the Bazett's formula (13), and called RV-SD4. Forty healthy controls, matched for age, sex, and body mass index (BMI), were included to define the normal range of RV-SD4.

To define intraobserver and interobserver variability, 2D speckle tracking echocardiography (STE) measurements were repeated for all patients by the same observer (B.R.) and by a second independent observer (R.M.).

STATISTICAL ANALYSIS. Continuous data are expressed as mean ± SD, and categorical data are expressed as counts and proportions. Two-group comparisons were performed with unpaired or paired 2-tailed Student *t* tests for means if the data were normally distributed or with Wilcoxon rank-sum tests if the data were not normally distributed. Chi-square or Fisher exact tests were used to analyze the categorical data.

Actuarial freedom from episodes of CW was determined by the Life Table method. Kaplan-Meier (product-limit) graphs were used to show CW over time. Patients who were without CW were censored on the date of the conclusion of the study.

Multivariate Cox regression models were constructed to identify risk factors for CW. First, a base model was generated that included variables significantly ($p < 0.05$) associated with CW on univariate analysis (age, sex, WHO class, 6MWT, and hemodynamic and echocardiographic parameters). A p value of 0.10 was the criterion to remove covariates from the model until the most parsimonious model was sought. A second comparative Cox model was used to assess the relative prognostic power of RV-SD4. The proportional-hazards assumptions were assessed with Durbin-Watson test.

The c-statistic was calculated for each model and compared by the method of DeLong et al. (14) to determine the incremental prognostic information of model-2.

A receiver operating characteristic (ROC) curve was used to test the ability of RV-SD4 to detect CW (optimal cutoff point highest and to the left on the ROC curve).

Regression analysis was performed to assess the relations between RV-SD4 and PVR changes during follow-up, identifying a quadratic model as the most accurate yet parsimonious.

For RV-SD4 measurement, intraobserver and interobserver variability was assessed by the Bland-Altman method: 0.10 ± 1.76 (95% confidence interval [CI]: -3.37 to +3.57) (average percentage variability 6.2%) and 0.14 ± 2.03 (95% CI: -3.85 to +4.13) (average percentage variability 7.2%), respectively, which can be considered acceptable for our clinical purpose (**Figure 1**).

FIGURE 1 Intraobserver and Interobserver Variability Assessed by the Bland-Altman Method

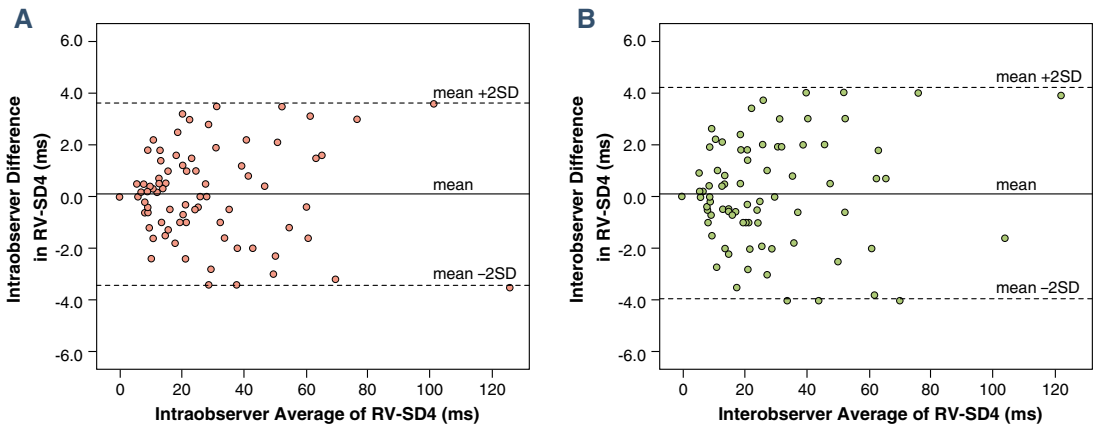

For RV-SD4 measurement, the difference in each pair of measurements was plotted against the pair's mean. **(A)** Intraobserver variability 0.10 ± 1.76 (95% CI: −3.37 to +3.57) (average percentage variability 6.2%). **(B)** Interobserver variability 0.14 ± 2.03 (95% CI: −3.85 to +4.13) (average percentage variability 7.2%). CI = confidence interval; RV = right ventricle; RV-SD4 = standard deviation of the times to peak-systolic strain for the 4 mid-basal right ventricular segments.

All statistical analyses were performed using SPSS software (version 20.0, IBM Corp. 2011, Milan, Italy) and MedCalc (version 13.3, 2013, Mariakerke, Belgium).

RESULTS

Baseline characteristics of the 80 PAH patients are summarized in Table 1. The majority of patients was female, WHO class III, with severe PAH and impaired effort capacity.

As expected, PAH patients presented impaired morphologic and systolic function echocardiographic parameters compared with control subjects (Table 2).

VARIABILITY OF RV DYSSYNCHRONY MODELS IN NORMAL SUBJECTS BY STE ANALYSIS. Analyzing the time to peak strain of the 6 RV segments among normal subjects, we observed a high variability of the apical segments of both the right ventricular free wall (RVFW) and the interventricular septum (IVS) compared with the mid and basal segments (395 ± 49 ms vs. 386 ± 33 ms and 384 ± 34 ms, respectively). Consequently, we found a higher standard deviation when RVD was quantified by the 6-segment model in respect to the 4-segment model (16 ± 10 ms vs. 9 ± 5 ms, respectively; p = 0.03), even if corrected to the R-R intervals (15 ± 9 ms vs. 8 ± 5 ms, respectively; p = 0.03).

RV DYSSYNCHRONY. The mean 2D strain value of the basal and medium segments of both the RVFW and the IVS were 21.2 ± 6.7%, 19.4 ± 7.0%, 18.4 ± 10.1%, and 16.9 ± 10.6%, respectively, with a delayed time to maximal deformation of the RVFW compared with the IVS (408 ± 61 ms vs. 376 ± 50 ms, respectively). RVD determined by RV-SD4 was 27 ± 23 ms in the patients group and 8 ± 5 ms in the control group. Using the upper 95% limit of normal (mean + 2SD) of the control group, we defined a cutoff value of 18 ms as criterion for RVD. According to this criterion, RVD was present in 48 patients (60%). An example of a normal subject (A) compared with a patient with significant RVD (B) is shown in Figure 2. As shown in

TABLE 1 Demographic, Clinical, and Hemodynamic Characteristics of the Study Population

Diagnosis	
Idiopathic PAH	71 (89)
Heritable PAH	5 (6)
Anorexigen-induced PAH	4 (5)
Sex, M/F	28/52
Age, yrs	57 ± 14
Weight, kg	68 ± 16
Height, cm	163 ± 9
Follow-up, days	416 ± 210
Functional class	
WHO II	28 (35)
WHO III	47 (59)
WHO IV	5 (6)
6MWT, m	429 ± 119
Hemodynamics	
RAP, mm Hg	7.8 ± 4.7
PAP, mm Hg	49 ± 15
Cardiac index, l/min/m^2	2.7 ± 0.7
PWP, mm Hg	9 ± 3
PVR, WU	10.1 ± 4.8
Compliance, ml/mm Hg	1.5 ± 1.1
QRS, ms	85 ± 14
First-line therapy	
Calcium-channel blockers	5 (6)
ERA	33 (41)
PDE5i	28 (35)
Epoprostenol	4 (5)
Treprostinil	10 (13)

Values are n (%), n, or mean ± SD.

6MWT = nonencouraged 6-min walk test; ERA = endothelin receptor antagonist; PAH = pulmonary arterial hypertension; PAP = mean pulmonary arterial pressure; PDE5i = phosphodiesterase 5 inhibitor; PVR = pulmonary vascular resistance; PWP = mean pulmonary wedge pressure; RAP = mean right atrial pressure; WHO = World Health Organization; WU = Wood Unit.

TABLE 2 Comparison of Echocardiographic Features Between PAH Patients and Normal Subjects

	Normal Subjects (N = 40)	PAH (N = 80)	p Value
Heart rate, beats/min	69 ± 12	76 ± 12	0.03
PVC, ms	399 ± 29	389 ± 37	ns
Morphological features			
RA area, cm^2	14 ± 2	30 ± 10	<0.00001
RVEDA, cm^2	14 ± 2	25 ± 7	<0.00001
RVESA, cm^2	7 ± 1	16 ± 7	<0.00001
LVEId	0.99 (0.99–1.01)	1.27 (1.16–1.50)	<0.0001
LVEIs	1.01 (0.99–1.05)	1.44 (1.20–1.73)	<0.0001
Pericardial effusion	0	25	<0.0001
RV systolic function			
RVFAC, %	53 ± 3	37 ± 11	<0.00001
TAPSE, mm	27 ± 2	20 ± 4	<0.00001
pTDI S1, cm/s	11.5 ± 2.4	8.4 ± 2.8	<0.0001
pTDI S2, cm/s	14.3 ± 2.2	11.0 ± 2.9	<0.0001
pTDI RV IVA, m/s^2	4.0 ± 0.6	2.7 ± 0.8	<0.00001
Peak 2DS mid RVFW, %	32.0 ± 4.8	19.4 ± 7.0	<0.00001
Peak 2DS basal RVFW, %	31.7 ± 6.8	21.2 ± 6.7	<0.00001
Intraventricular dyssynchrony			
RV-SD4, ms	8 ± 5	27 ± 23	<0.00001

Values are mean ± SD, median (interquartile range), or n.

2DS basal RVFW = 2-dimensional strain of the basal segment of the RVFW by Speckle-Tracking Echocardiography; 2DS mid RVFW = 2-dimensional strain of the mid segment of the RVFW by Speckle-Tracking Echocardiography; IVA = isovolumic acceleration; LVEId = left ventricular end-diastolic eccentricity index; LVEIs = left ventricular end-systolic eccentricity index; PAH = pulmonary arterial hypertension; pTDI RV IVA = right ventricular isovolumic acceleration; pTDI S1 = pulsed tissue Doppler peak isovolumic velocity at the basal RVFW segment; pTDI S2 = pulsed tissue Doppler peak systolic velocity at the basal RVFW segment; PVC = pulmonary valve closure; RA = right atrium area; RV = right ventricular; RVEDA = right ventricular end-diastolic area; RVESA = right ventricular end-systolic area; RVFAC = right ventricular fractional area change; RVFW = right ventricular free wall; RV-SD4 = standard deviation of the times to peak-systolic strain for the 4 mid-basal RV segments; TAPSE = tricuspid annular plane systolic excursion.

JACC: CARDIOVASCULAR IMAGING, VOL. 8, NO. 6, 2015
JUNE 2015:642–52

FIGURE 2 Example of RVD Evaluation by STE in a Normal Subject and in a Patient With Significant RVD

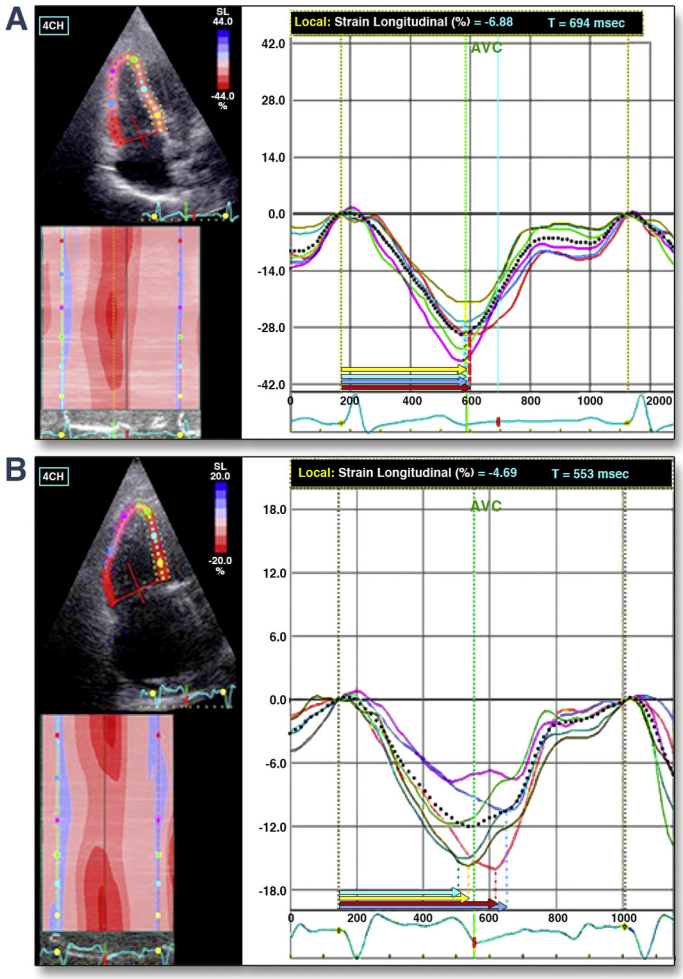

(A) Normal subject. **(B)** Patient with significant RVD by STE. The **colored lines** represent the time-interval between QRS onset and peak systolic strain for each RV segment for RV-SD4 measurement (**red line**: basal RVFW; **blue line**: mid RVFW; **yellow line**: basal IVS; **light-blue line**: mid IVS). AVC = aortic valve closure; IVS = interventricular septum; RV = right ventricle; RVD = right ventricular dyssynchrony; RVFW = right ventricular free wall; STE = speckle tracking echocardiography; other abbreviation as in Figure 1.

TABLE 3 Comparison of Clinical, Echocardiographic, and Hemodynamic Characteristics of PAH Patients Based on RV-SD4 >2 SD UNL

	RV-SD4 ≤18 (n = 32)	RV-SD4 >18 (n = 48)	p Value
Age, yrs	56 ± 15	57 ± 15	NS
Weight, kg	65 ± 16	70 ± 15	NS
Height, cm	163 ± 10	163 ± 9	NS
Sex, M/F	8/24	16/32	NS
QRS, ms	81 ± 14	83 ± 15	NS
WHO	2.4	2.9	<0.0001
6MWT, m	472 ± 104	401 ± 120	<0.007
Hemodynamics			
RAP, mm Hg	6.6 ± 3.9	8.6 ± 5.0	0.06
PAP, mm Hg	45 ± 13	50 ± 15	NS
PWP, mm Hg	10.0	9.6	NS
Cardiac index, l/min/m^2	3.0 ± 0.7	2.5 ± 0.8	0.007
PVR, WU	7 ± 3	10 ± 5	0.006
Echocardiography			
Heart rate, beats/min	76 ± 10	75 ± 13	NS
PVC, ms	391 ± 31	388 ± 41	NS
RA area, cm^2	25 ± 7	33 ± 11	0.0007
RVEDA, cm^2	21 ± 7	28 ± 7	0.0001
RVESA, cm^2	13 ± 6	18 ± 6	0.0004
RVFAC, %	40 ± 11	36 ± 11	0.06
TAPSE, mm	21 ± 3	19 ± 4	NS
LVEId	1.22 (1.08–1.39)	1.29 (1.19–1.60)	0.01
LVEIs	1.24 (1.15–1.56)	1.55 (1.26–1.90)	0.003
Pericardial effusion	3 (9)	21 (43)	<0.0001
pTDI S1, cm/s	9.2 ± 3.1	7.9 ± 2.5	0.06
pTDI S2, cm/s	11.1 ± 2.3	11.1 ± 3.3	NS
pTDI RV IVA, m/s^2	3.1 ± 0.7	2.5 ± 0.7	0.001
Peak 2DS mid RVFW, %	22 ± 6	18 ± 7	0.002
Peak 2DS basal RVFW, %	22 ± 7	20 ± 6	NS
Systolic shortening time, ms	311 ± 48	340 ± 45	0.04
Post-systolic shortening, ms	−5 ± 38	38 ± 49	0.001

Values are mean ± SD, n, median (interquartile range), or n (%).
UNL = upper normal limit; other abbreviations as in Tables 1 and 2.

Table 3, analyzing the clinical, hemodynamic, and echocardiographic profiles of the 2 groups of patients divided by the 95% upper limit value of the normal population of RV-SD4 (18 ms), the 2 groups were comparable for demographic characteristics. Patients with RVD had a more advanced WHO functional class, worse exercise tolerance, and more impaired hemodynamic condition compared to patients ≤18 ms. Those patients also had worse RV morphological remodeling and more frequently pericardial effusion compared to the other patients, but similar RV systolic function. Notably, in patients with RV-SD4 >18 ms, RV mid- and basal-segment shortening time occurred 38 ± 49 ms after pulmonary valve closure, representing 10 ± 13% of the entire shortening time (340 ± 45 ms).

FACTORS INFLUENCING RV DYSSYNCHRONY. We performed a stepwise backward multivariate regression analysis to determine the most important RV morphologic, electrical, and hemodynamic parameters influencing right intraventricular mechanical

delay. PVR (unstandardized coefficient B 1.76, odds ratio [OR]: 5.9; p = 0.006), RVEDA (unstandardized coefficient B 0.96, OR: 2.6; p = 0.002), and QRS duration (unstandardized coefficient B 0.36, OR: 1.4; p = 0.02) were found to be independent predictors of intraventricular delay (r = 0.62; r^2 = 0.38; p < 0.000001).

RV DYSSYNCHRONY AND CLINICAL WORSENING. In the overall cohort, after a median follow-up of 297 ± 102 days, 26 of 80 patients presented with CW (32.5%). Actuarial rates of CW were 19% at 6 months and 31% at 1 year. Mean time to CW was 170 ± 83 days.

No significant differences were observed between patients with and without CW regarding demographic profile (Table 4). As expected, the former group had worse WHO functional class, 6MWT, hemodynamic impairment, RV remodeling, and dysfunction compared with patients without CW. Notably, the average RV-SD4 among event-free survivors was 19 ± 13 ms versus 45 ± 27 ms among patients who presented CW (p < 0.0001). Twenty-four of 26 events (92.3%) occurred in patients with an RV-SD4 greater than 18 ms.

Cox regression model 1 for CW prediction was constructed with those variables significantly resulting from univariate analysis excluding RV-SD4 (Table 5). Among demographic, clinical, hemodynamic, and echocardiographic parameters, WHO functional class IV, 6MWT, and cardiac index remained independent predictors of CW (model 1: 0.74, 95% CI: 0.62 to 0.85; p = 0.001) (Table 6). Adding the RV-SD4 to model 1, we observed a significant improvement in c-statistics (model 2: 0.81, 95% CI: 0.70-0.91; p = 0.0001) showing an improvement in the prognostic power (0.81 vs. 0.74; 95% CI: 0.02 to 0.11; p = 0.005) (Figure 3).

The ROC analysis identified a baseline RV-SD4 of 23 ms as the best cutoff value for CW prediction (area under the curve 0.85, 95% CI: 0.75 to 0.93; SE 0.045). An RV-SD4 of 23 ms showed 92% sensitivity, 63% specificity, and a high negative predictive value of 95% (positive predictive value 57%) for adverse outcomes.

The 6-month and 1-year event-free survival estimates were 88% and 85%, respectively, for patients with an RV-SD4 <23 ms compared with 62% and 45%, respectively, for patients with a RV-SD4 ≥23 ms (Figure 4).

RV DYSSYNCHRONY EVOLUTION. At 12 months, patients without CW experienced a significant improvement in WHO functional class, exercise tolerance, all hemodynamic parameters, and RV chamber morphological parameters (Table 7). In these patients, RVD significantly decreased at second evaluation compared to baseline (19.57 ± 14.0 ms vs. 14.96 ± 10.0 ms, respectively; p = 0.001). Interestingly, a significant relationship was found between RV-SD4 improvement and RVEDA reduction (r^2 = 0.52; p = 0.001; y = -2.8 + 2.0x) and PVR decrease, with those patients with the greatest reduction of PVR showing a complete normalization of RV-SD4 (r^2 = 0.59; p = 0.0001; $y = 4.1 + 0.2x - 0.007x^2$) (Figure 5). Indeed, 10 patients showed complete regression of RVD associated with a 42 ± 4% reduction of PVR. On the contrary, at the time of CW, patients presented a significant increase of RV-SD4 compared to baseline (49.75 ± 26.00 ms vs. 45.40 ± 28.00 ms, respectively; p = 0.01) and to those patients without CW (+4.61 ms vs. -4.35 ms, respectively; p = 0.0001). This increase in RVD was coupled with a 15 ± 12% increase in PVR, no significant modification of cardiac index and right

TABLE 4 Comparison of Clinical, Echocardiographic, and Hemodynamic Characteristics of the Overall Cohort Based on Clinical Worsening

	No CW (n = 54)	CW (n = 26)	p Value
Age, yrs	56 ± 16	59 ± 14	NS
Weight, kg	67 ± 15	72 ± 18	NS
Height, cm	164 ± 10	161 ± 7	NS
Sex, M/F	18/36	6/20	NS
QRS, ms	81 ± 14	85 ± 16	NS
WHO	2.5 ± 0.5	3.2 ± 0.4	<0.0001
6MWT, m	475 ± 102	334 ± 94	<0.0001
Hemodynamics			
RAP, mm Hg	6.5 ± 3.3	11.2 ± 5.3	<0.0001
PAP, mm Hg	44 ± 13	55 ± 13	<0.001
Cardiac index, l/min/m^2	3.0 ± 0.7	2.0 ± 0.5	<0.0001
PVR, WU	7 ± 3	13 ± 5	<0.0001
Echocardiography			
Heart rate, beats/min	74 ± 11	80 ± 13	0.04
PVC, ms	398 ± 29	372 ± 46	0.003
RA area, cm^2	26 ± 7	39 ± 11	<0.0001
RVEDA, cm^2	23 ± 7	30 ± 7	0.0001
RVESA, cm^2	14 ± 6	21 ± 7	<0.0001
RVFAC, %	41 ± 10	31 ± 10	<0.0001
TAPSE, mm	21 ± 3	18 ± 4	<0.001
LVEId	1.21 (1.08–1.32)	1.56 (1.27–2.07)	0.0001
LVEIs	1.25 (1.15–1.57)	1.81 (1.50–2.19)	0.0001
Pericardial effusion	12 (22)	13 (50)	0.001
pTDI S1, cm/s	9.2 ± 2.7	6.9 ± 2.6	<0.001
pTDI S2, cm/s	11.6 ± 2.4	10.0 ± 3.6	0.02
pTDI RV IVA, m/s^2	3.0 ± 0.7	2.2 ± 0.6	<0.0001
Peak 2DS mid RVFW, %	22 ± 6	15 ± 5	<0.0001
Peak 2DS basal RVFW, %	23 ± 6	17 ± 6	<0.0001
Systolic shortening time, ms	324 ± 49	339 ± 65	NS
Post-systolic shortening, ms	3 ± 41	48 ± 52	0.0001
RV-SD4, ms	19 ± 13	45 ± 27	<0.0001

Values are mean ± SD, n, median (interquartile range), or n (%).
CW = clinical worsening; other abbreviations as in Tables 1 and 2.

JACC: CARDIOVASCULAR IMAGING, VOL. 8, NO. 6, 2015
JUNE 2015:642–52

TABLE 5 Univariate Analysis of Clinical, Echocardiographic, and Hemodynamic Variables Associated With Clinical Worsening

	Unit	HR	95% CI	p Value
Age, yrs	1	1.01	0.98–1.04	NS
Sex		0.70	0.28–1.74	NS
WHO	1	6.6	3.30–13.2	<0.0001
6MWT, m	1	0.99	0.98–0.99	<0.0001
Hemodynamics				
Mean PAP, mm Hg	1	1.06	1.03–1.09	<0.0001
RAP, mm Hg	1	1.16	1.08–1.24	<0.0001
Cardiac index, l/min/m^2	1	0.12	0.06–0.25	<0.0001
PVR, WU	1	1.28	1.18–1.39	<0.0001
Echocardiography				
RA area, cm^2	1	1.08	1.05–1.11	<0.0001
LVEId	1	10.3	4.23–25.03	<0.0001
LVEIs	1	3.41	2.17–5.33	<0.0001
RVEDA, cm^2	1	1.08	1.04–1.13	<0.0001
RVESA, cm^2	1	1.11	1.06–1.17	<0.0001
RVFAC, %	1	0.92	0.88–0.96	<0.0001
TAPSE, mm	1	0.84	0.76–0.92	<0.0001
Pericardial effusion		2.73	1.26–5.91	0.011
pTDI S1, cm/s	1	0.77	0.65–1.11	NS
pTDI S2, cm/s	1	0.86	0.75–1.06	NS
pTDI RV IVA, m/s^2	1	0.24	0.12–0.46	<0.0001
Peak 2DS mid RVFW, ms	1	0.87	0.82–0.93	<0.0001
Peak 2DS basal RVFW, ms	1	0.85	0.79–0.91	<0.0001
RV-SD4, ms	1	1.03	1.01–1.03	<0.0001

CI = confidence interval; HR = hazard ratio; other abbreviations as in Tables 1 and 2.

FIGURE 3 Comparison of the ROC Curves for Prediction of Clinical Worsening Between the Baseline Model and the Model Containing RV-SD4

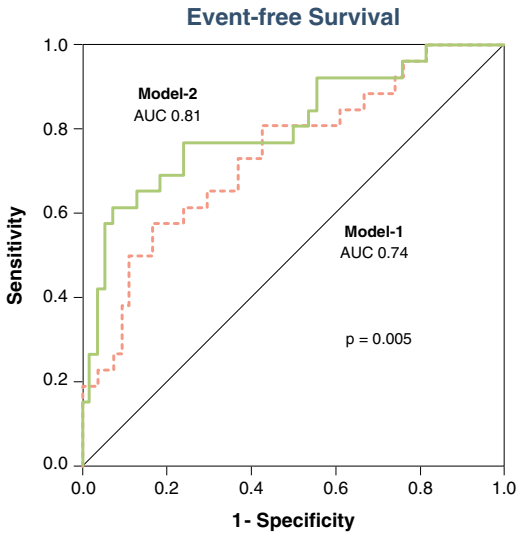

Baseline model is model 1 **(pink dashed line)**, and the model containing RV dyssynchrony (RV-SD4) is Model 2 **(green solid line)**. A significant improvement in accuracy is observed for model 2 in predicting clinical worsening (0.74 vs. 0.81; p = 0.005; 95% CI: 0.02 to 0.11). AUC = area under the curve; ROC = receiver operating characteristic; other abbreviations as in Figure 1.

atrial pressure, and worsening of RV remodeling parameters.

DISCUSSION

This is the first prospective study in a large series of consecutive IPAH, HPAH, and APAH therapy-naïve patients that shows: 1) the high prevalence of RVD, as already described in pediatric PAH patients (15); 2) the major determinants of RVD as increased afterload, morphologic RV remodeling, and to a lesser extent QRS duration; 3) RVD as an independent prognostic factor together with WHO functional class IV, 6MWT, and cardiac index; and 4) the reversibility of RVD when a large reduction of PVR is achieved.

TABLE 6 Cox Regression Models for Clinical Worsening Prediction

	Unit	HR	(95% CI)	p Value	c-Statistic (95% CI)
Model 1					0.74 (0.62–0.85)
WHO IV		5.7	(1.19–27.9)	0.02	
6MWT	1	0.99	(0.98–0.99)	0.001	
Cardiac index	1	0.13	(0.05–0.30)	0.0001	
Model 2					0.81 (0.70–0.91)
WHO IV		13.9	(2.13–92.0)	0.006	
6MWT	1	0.99	(0.98–0.99)	0.001	
Cardiac index	1	0.13	(0.05–0.35)	0.0001	
RV-SD4 ≥23 ms		3.8	(1.34–11.0)	0.01	

Model 1 (chi-square = 49.37; df = 3; p < 0.0001); model 2 (chi-square = 57.02; df = 4; p < 0.0001)

df = degrees of freedom; WHO IV = WHO functional class IV; other abbreviations as in Tables 1, 2, and 3.

In comparison with previous studies, our population consisted of a large homogeneous cohort of naïve patients representative of the whole spectrum of the disease stages and in the absence of confounding factors. The few studies available on this issue have been considering only smaller samples of prevalent pulmonary hypertension patients with possible confounding factors such as associated PAH disease and other comorbidities (4–6,16).

RV DYSSYNCHRONY MODELS BY STE ANALYSIS. In contrast to conventional tissue Doppler imaging (TDI), angle independence and an improved signal-to-noise ratio are the main advantages of the STE method to overcome limitations in the assessment of strain values (11). Furthermore, longitudinal strain

analysis by STE has been found to reflect the systolic myocardial contractile delay more accurately than using the wall velocities, as with TDI (11).

The higher variability of the time-to-peak strain of the apical segments found in normal subjects can be explained by several technical limitations (11,17,18): image quality related to near-field artifacts; inadequate frame rate due to the wide sector angle that is necessary to visualize the entire remodeled RV apex; the assumption that morphologic details can be tracked from one frame to the next, which may not be true for the RV apical segments where out-of-plane motion occurs; STE is not completely angle independent, presenting worse resolution for the remodeled RV apex. For these technical reasons we have excluded RV apical segments for RVD evaluation as the results appeared to be inconsistent.

DETERMINANTS OF RV DYSSYNCHRONY. Our findings clearly indicate that in IPAH, HPAH, and APAH, RVD is mainly explained by the combined effect of increased PVR, RV chamber dilation, and QRS duration. These 3 factors may contribute to dyssynchronous RV wall motion with several pathophysiological mechanisms.

Data are available from the large experience in left heart disease showing that an increased afterload plays an important role as a cause of LV dyssynchrony even in the presence of narrow QRS complexes (19,20). Indeed, afterload per se seems to induce LV dyssynchrony in normal subjects during a pharmacological challenge in the absence of other confounding factors (21). In PAH patients, it has been shown that RV wall stress correlates with regional differences in the duration of contraction between the RV FW and left ventricular lateral wall, measuring times-to-peak myocardial shortening by magnetic resonance imaging (6). Thus, nonuniform distribution of regional myocardial wall stress is very likely a major determinant of RVD. Moreover, the interplay between RV dilation and afterload in inducing RVD has been documented in animal models in which RV dilation, induced by increased afterload, has been associated with changes in RV action potential

FIGURE 4 Event-Free Survival of Patients With a RV-SD4 ≥23 ms Compared to Patients With a RV-SD4 <23 ms

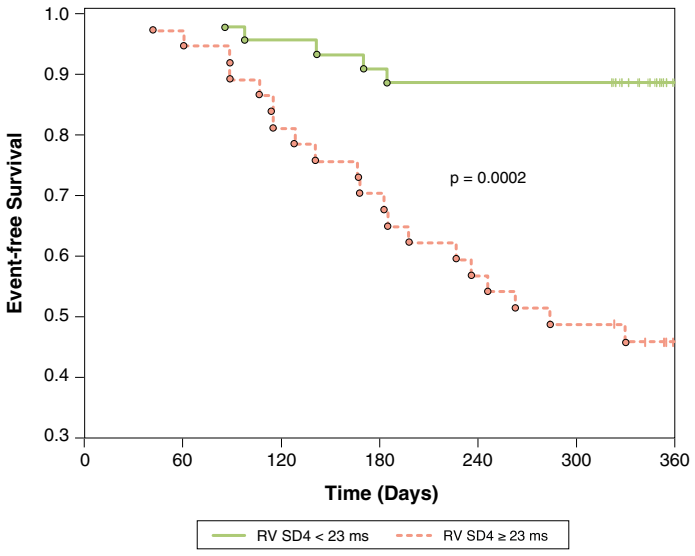

Abbreviations as in Figure 1.

TABLE 7 Differences During Follow-Up in Clinical, Hemodynamic, RV Morphological Parameters, and RVD Between Patients With and Without Clinical Worsening

	Clinical Worsening				No Clinical Worsening			
	Basal	12 months	Δ	p Value	Basal	12 months	Δ	p Value
WHO	3.1 ± 0.3	3.2 ± 0.3	+0.1 ± 0.3	NS	2.4 ± 0.5	1.8 ± 0.3	-0.6 ± 0.5	0.0001
6MWT, m	367 ± 68	326 ± 73	-42 ± 28	0.0001	476 ± 99	508 ± 77	+32 ± 33	0.0001
PAP, mm Hg	56 ± 14	58 ± 12	+2 ± 4	0.03	45 ± 13	38 ± 11	-7 ± 7	0.0001
RAP, mm Hg	9 ± 5	10 ± 4	+0.8 ± 1.9	NS	6 ± 3	5 ± 1	-1.3 ± 2.6	0.001
Cardiac index, l/min/m^2	2.0 ± 0.4	1.9 ± 0.3	-0.06 ± 0.2	NS	3.0 ± 0.6	3.1 ± 0.5	+0.1 ± 0.2	0.001
PVR, WU	13.8 ± 5.5	15.3 ± 5.0	+1.5 ± 1.3	0.0001	7.2 ± 3	5.6 ± 2.0	-1.6 ± 1.2	0.0001
RA area, cm^2	37 ± 10	39 ± 9	+1.5 ± 2.2	0.007	26 ± 7	24 ± 6	-1.2 ± 2.0	0.0001
LVEId	1.56 (1.27 to 2.07)	1.56 (1.40 to 1.90)	0.05 (-0.39 to 0.19)	0.001	1.21 (1.08 to 1.32)	1.16 (1.09 to 1.25)	-0.01 (-0.07 to 0.00)	0.001
LVEIs	1.81 (1.50 to 2.19)	1.90 (1.62 to 2.47)	0.09 (-0.38 to 0.28)	0.0001	1.25 (1.15 to 1.57)	1.19 (1.12 to 1.41)	-0.04 (-0.12 to 0.01)	0.0001
RVEDA, cm^2	30 ± 8	34 ± 6.5	+3.8 ± 2.8	0.0001	23 ± 7	22 ± 6	-1.0 ± 2.7	0.01
RVESA, cm^2	21 ± 6	25 ± 6.5	+4 ± 2.7	0.0001	14 ± 6	12 ± 5	-1.2 ± 2.7	0.002
RV-SD4, ms	45.40 ± 28	49.75 ± 26	+4.61 ± 9.3	0.01	19.57 ± 14	14.96 ± 10	-4.35 ± 7.6	0.001

Values are mean ± SD.

RVD = right ventricular dyssynchrony; other abbreviations as in Tables 1, 2, and 3.

FIGURE 5 Correlation Between the Changes in RV-SD4 and PVR During Follow-Up

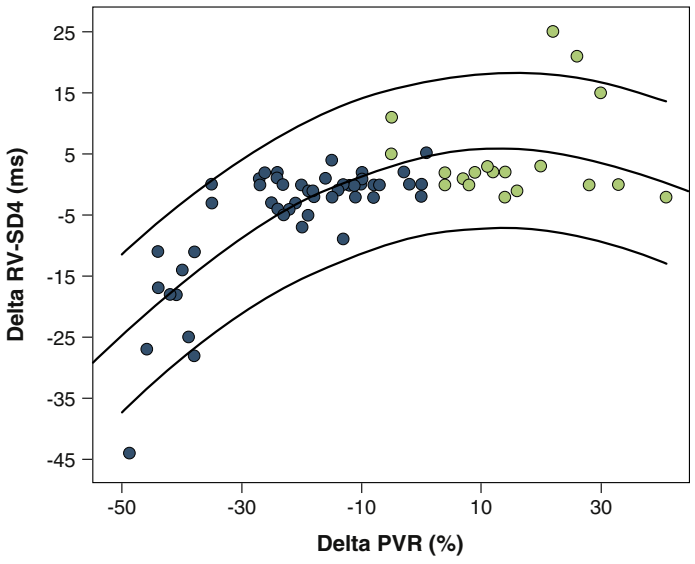

Quadratic model: $r^2 = 0.59$, $p = 0.0001$, $y = 4.1 + 0.21x - 0.007x^2$; linear model: $r^2 = 0.44$, $p = 0.0001$, $y = 1.39 + 0.31x$. Patients with and without clinical worsening are reported in the same scatterplot (**green circles and blue circles**, respectively). PVR = pulmonary vascular resistance; other abbreviations as in Figure 1.

duration and conduction properties by altering cell-to-cell coupling (22). Similar results have been found by Hardziyenka et al. (16) in chronic thromboembolic pulmonary hypertension patients, confirming that increased RV size is a contributing factor to interventricular delay by electrophysiological epicardial mapping during pulmonary endarterectomy.

Finally, not surprisingly, we found that QRS duration is the third independent factor for RVD, although multivariate analysis confers the prevalent role to PVR and RV dilation. This finding is in contrast to Kalogeropoulos et al. (5), who failed to show a significant correlation between RVD and QRS duration, but that study included a smaller and more heterogeneous population of PAH patients, making those findings quite inconsistent.

In this pathophysiologic condition, RVD means that the late phase of RV contraction may not contribute to stroke volume (i.e., post-systolic shortening). In patients with RVD, post-systolic shortening was 10 ± 13% of total RV shortening, reaching up to 17 ± 9% in those with RVD >23 ms (range 3% to 31%). According to our results, inefficient RV shortening may facilitate cardiac index reduction, despite no significant differences of most RV systolic function parameters between patients with and without RVD. This is in agreement with and extends the findings of Marcus et al. (6) who observed a negative correlation between prolonged RV shortening and RV stroke volume.

PREDICTORS OF CLINICAL WORSENING. It is widely accepted that RV function is the primary determinant of prognosis in PAH. Our results confirm the prognostic relevance of WHO functional class IV, 6MWT, and cardiac index, directly related to RV function, and identify RVD as a new independent prognostic factor.

WHO functional class IV, 6MWT, and cardiac index have been historically associated with prognosis since before modern treatments were available (23), and the importance of these parameters has been confirmed in modern registries, such as the French and the Reveal registry (8,24), emphasizing invasive hemodynamic evaluation as mandatory in all PAH naïve patients.

Furthermore, we documented for the first time that RVD is an independent predictor of unfavorable clinical events in IPAH, HPAH, and APAH patients. Patients with RV-SD4 ≥23 ms have a 3.8-fold increased risk of CW on long-term follow-up. RV-SD4 evaluation added significant prognostic information to well-established clinical, hemodynamic, and echocardiographic data, as shown by the incremental value of the c-statistic. Interestingly, almost all the patients without CW in our cohort had an RV-SD4 below the normal limit (18 ms) at the time of diagnosis, emphasizing the potential role in clinical practice. Because of its high negative predictive value, physicians could be reassured on a more favorable course of the disease for those patients without RVD at diagnosis, especially if matching with other well-known predictive functional and hemodynamic variables.

RV DYSSYNCHRONY EVOLUTION. Our findings show for the first time that RVD in PAH can be reversed by a remarkable decrease in PVR. As can be seen in Figure 5, a nonlinear relationship is present between RV-SD4 and PVR, showing a significant decrease in RVD when large PVR reduction can be reached and allowing full normalization in 10 patients. Such hemodynamic improvement is associated with a significant reduction of RV dilation related to RV-SD4 reduction, contributing to normal restoration of RV shortening times.

Follow-up data confirm the important role of PVR and RV size on determining RVD, emphasizing how RV wall stress could be the common denominator affecting RV regional differences in shortening time.

STUDY LIMITATIONS. Our study cohort consisted of patients referred to a single tertiary center, which

might constitute a referral bias. However, this is a common limitation of similar studies.

The second limitation is that the duration of disease may influence the development of RVD, its reversibility, and patient prognosis. However, determining the onset and duration of disease in PAH is challenging. We are therefore unable to evaluate its influence on RVD.

Another limitation arises from a possible type I error inflation given the multiple screened predictors in light of the relatively small number of patients with events.

Finally, a possible technical limitation comes from STE analysis, which requires a training period and experience to achieve reproducible results. Two specific limitations of STE are the need of good image acquisition to obtain adequate endocardial border delineation and the inability to use this technique in nonsinus rhythms (25).

CONCLUSIONS

The results of the present study extend the sparse data on RVD, defining a robust pathophysiologic model of RVD determining factors, which emerged as the combination of PVR, RVEDA, and QRS duration. This model may provide further insight into the understanding of RV adaptation to increased afterload in IPAH, HPAH, and APAH.

The most important findings of our study are the demonstration of the independent prognostic impact of RV-SD4 as a new noninvasive parameter with high negative predictive value and the possibility of RVD regression for large decreases in PVR with PAH therapies. Our findings should be confirmed in a larger multicenter trial focusing on changes in RVD during targeted PAH therapy and its impact on survival.

ACKNOWLEDGMENTS The authors thank Lewis J. Rubin and Stefano Ghio for the critical review of the manuscript.

REPRINT REQUESTS AND CORRESPONDENCE TO: Dr. Roberto Badagliacca, Department of Cardiovascular and Respiratory Science, I School of Medicine, Sapienza University of Rome, Policlinico Umberto I, Viale del Policlinico 155, 00161 Rome, Italy. E-mail: roberto.badagliacca@uniroma1.it.

PERSPECTIVES

COMPETENCY IN MEDICAL KNOWLEDGE: Prognosis in PAH depends on the ability of the RV to maintain its function in the face of increased afterload. RVD has been described in PAH, but no evidence is available on its prognostic impact and evolution after therapy.

COMPETENCY IN PATIENT CARE: RVD is not uncommon in pulmonary arterial hypertension, it might regress during effective treatments and represents a noninvasive parameter with an independent prognostic impact on clinical worsening, increasing the prognostic power of the model based on traditional clinical, hemodynamic, and echocardiographic parameters.

TRANSLATIONAL OUTLOOK: The results of this study should be confirmed in a larger, multicenter trial focusing on changes in RVD during targeted PAH therapy, and its impact on survival.

REFERENCES

1. Kawut SM, Al-Naamani N, Agerstrand C, et al. Determinants of right ventricular ejection fraction in pulmonary arterial hypertension. Chest 2009;135:752–9.

2. Voelkel NF, Quaife RA, Leinwand LA, et al. Right ventricular function and failure: report of a National Heart, Lung, and Blood Institute working group on cellular and molecular mechanisms of right heart failure. Circulation 2006;114:1883–91.

3. Cleland JG, Daubert JC, Erdmann E, et al., Cardiac Resynchronization-Heart Failure (CARE-HF) Study Investigators. The effect of cardiac resynchronization on morbidity and mortality in heart failure. N Engl J Med 2005;352:1539–49.

4. Lopez-Candales A, Dohi K, Bazaz R, Edelman K. Relation of right ventricular free wall mechanical delay to right ventricular dysfunction as determined by tissue Doppler imaging. Am J Cardiol 2005;96:602–6.

5. Kalogeropoulos AP, Georgiopoulou VV, Howell S, et al. Evaluation of right intraventricular dyssynchrony by two-dimensional strain echocardiography in patients with pulmonary arterial hypertension. J Am Soc Echocardiogr 2008;21:1028–34.

6. Marcus JT, Gan CT, Zwanenburg JJ, et al. Interventricular mechanical asynchrony in pulmonary arterial hypertension: left-to-right delay in peak shortening is related to right ventricular overload and left ventricular underfilling. J Am Coll Cardiol 2008;51:750–7.

7. Galiè N, Hoeper MM, Humbert M, et al., ESC Committee for Practice Guidelines (CPG). Guidelines for the diagnosis and treatment of pulmonary hypertension: the Task Force for the Diagnosis and Treatment of Pulmonary Hypertension of the European Society of Cardiology (ESC) and the European Respiratory Society (ERS), endorsed by the International Society of Heart and Lung Transplantation (ISHLT). Eur Heart J 2009;30:2493–537.

8. Humbert M, Sitbon O, Chaouat A, et al. Survival in patients with idiopathic, familial, and anorexigen-associated pulmonary arterial hypertension in the modern management era. Circulation 2010;122:156–63.

9. McLaughlin VV, Badesch DB, Delcroix M, et al. End points and clinical trial design in pulmonary arterial hypertension. J Am Coll Cardiol 2009;54 Suppl 1:S97–107.

10. Vizza CD, Yusen RD, Lynch JP, Fedele F, Patterson GA, Trulock EP. Outcome of patients with cystic fibrosis awaiting lung transplantation. Am J Respir Crit Care Med 2000;162:819–25.

11. Rudski LG, Lai WW, Afilalo J, et al. Guidelines for the echocardiographic assessment of the right heart in adults: a report from the American Society of Echocardiography. Endorsed by the European Association of Echocardiography, a registered branch of the European Society of Cardiology, and the Canadian Society of

Echocardiography. J Am Soc Echocardiogr 2010; 23:685–713.

12. NTNU-Trondheim Norwegian University of Science and Technology Strain rate imaging. Available at: www.ntnu.edu/isb/echocardiography. Accessed June 1, 2014.

13. Bazett HC. An analysis of the time-relations of electrocardiograms. Heart 1920;7:353–70.

14. DeLong ER, DeLong DM, Clarke-Pearson DL. Comparing the areas under two or more correlated receiver operating characteristic curves: a nonparametric approach. Biometrics 1988;44:837–45.

15. Hill AC, Maxey DM, Rosenthal DN, et al. Electrical and mechanical dyssynchrony in pediatric pulmonary hypertension. J Heart Lung Transplant 2012;31:825–30.

16. Hardziyenka M, Campian ME, Bouma BJ, et al. Right-to-left ventricular diastolic delay in chronic thromboembolic pulmonary hypertension is associated with activation delay and action potential prolongation in right ventricle. Circ Arrhythmia Electrophysiol 2009;2:555–61.

17. Mor-Avi V, Lang RM, Badano LP, et al. Current and evolving echocardiographic techniques for the quantitative evaluation of cardiac mechanics: ASE/EAE consensus statement on methodology and indications. Endorsed by the Japanese Society of Echocardiography. Eur J Echocardiogr 2011;12: 167–205.

18. Gorcsan J III, Tanaka H. Echocardiographic assessment of myocardial strain. J Am Coll Cardiol 2011;58:1401–13.

19. Miura T, Bhargava V, Guth BD, et al. Increased afterload intensifies asynchronous wall motion and impairs ventricular relaxation. J Appl Physiol 1993;75:389–96.

20. Abe H, Nakatani S, Kanzaki H, et al. Effects of aortic valve replacement on left ventricular dyssynchrony in aortic stenosis with narrow QRS complex. J Am Soc Echocardiogr 2011; 24:1358–64.

21. Miyoshi H, Oishi Y, Mizuguchi Y, et al. Left ventricular systolic asynchrony is induced even in the normal heart during increases in afterload: a study with angiotensin II stress pulsed tissue Doppler imaging. J Echocardiogr 2007;5:41–7.

22. Lee JK, Kodama I, Honjo H, Anno T, Kamiya K, Toyama J. Stage-dependent changes in membrane currents in rats with monocrotaline-induced right ventricular hypertrophy. Am J Physiol 1997;272:H2833–42.

23. D'Alonzo GE, Barst RJ, Ayres SM, et al. Survival in patients with primary pulmonary hypertension. Ann Intern Med 1991;115:343–9.

24. Benza RL, Miller DP, Gomberg-Maitland M, et al. Predicting survival in pulmonary arterial hypertension: insights from the Registry to Evaluate Early and Long-Term Pulmonary Arterial Hypertension Disease Management (REVEAL). Circulation 2010;122:164–72.

25. Mondillo S, Galderisi M, Mele D, et al. Speckle-tracking echocardiography—a new technique for assessing myocardial function. J Ultrasound Med 2011;30:71–83.

KEY WORDS clinical worsening, pulmonary arterial hypertension, right ventricular dyssynchrony, right ventricular function